LED lamp flicker assessment under distorted grid voltage in both harmonic and supraharmonic ranges

Marwa S. Osheba, Abdellatif M. Aboutaleb, Jan Desmet, Senior Member, IEEE, and Jos Knockaert ,Senior Member, IEEE

***Abstract*—Supraharmonic background distortions are blamed for light flickers produced from LED lamps with no clear evidence in literature. Consequently, this paper is structured to investigate the effect of the background distortions in the harmonic and supraharmonic ranges on the light flickers produced from low power LED lamps that are widely used in residential applications. Four scenarios are performed: The first and second scenarios are done by exposing the LED lamp to a background distortion with harmonic and interharmonic voltage components, respectively. The third and fourth scenarios explore the impact of the grid voltage distortion in the supraharmonic range with frequencies that are integer and non-integer multiples of the grid frequency, respectively, on LED lamp flickers. The conducted study comes to the conclusion that visible flicker only appears for scenario 2, in which the visible flicker effect is in inverse relationship with the interharmonic frequencies. In both scenarios 1 and 3, no visible flicker is detected. In scenario 4, the light flicker is negligible. The observations are carried out experimentally on a commercial LED lamp. Then a mathematical analysis is provided to explain the observations in the four scenarios. The main outcomes are validated through a simulation study.**

***Index Terms*— electromagnetic compatibility, electromagnetic interference, harmonics, interharmonics, LED lamp drivers, light flickers, supraharmonics.**

I. INTRODUCTION

A. Interharmonics and Supraharmonics

Supraharmonic (SH) range, defined between $2\ kHz$ and $150\ kHz$, attracts the attention of the science society in order to recognize the problems and to convince the standardization committees to include limits to the power quality standards [1,2]. SHs are generated non-intentionally by switching grid-connected converters (GCCs) such as grid connected inverters (GCIs) [3,4], switched mode power supplies (SMPSs) [5,6], electric vehicle (EV) battery chargers [7], etc.

Many research has been conducted to identify the origin of the emissions in the SH range, the propagation and penetration of SHs in the grid, the problems associated with SHs existence in the grid, and others. The emissions in that range appear as sidebands around the switching frequencies and their integer multiples depending on both the grid and the switching frequencies. The low frequency (LF) harmonics below 2 kHz are related only to the grid frequency. This is because the SHs emissions are produced by the self-commutated converters, while the low frequency harmonics, below 2 kHz, are produced by line commutated converters and non-linear loads. LF interharmonics are mainly related to ripple control signals.

The propagation behavior of the SHs is different from the LF harmonics. While the LF harmonics tend to propagate into the grid, the SHs tend to propagate among the grid and the neighboring devices based on the grid and the neighboring devices impedance. The effect of the impedances of the low voltage (LV) cables on the SH propagation is investigated in [8]. The study in [8] is performed for a system that consists of a parallel connection of a LED lamp system and PV GCI. It is concluded that the LV grid installation, among the LED lamps, PV GCI and the grid, affects the SH propagation through the system.

Many problems are reported due to the existence of SH in LV grid, e.g., equipment malfunctions, unintentional switching, audible noise, electrical thermal stress, and reduction of the life-time [9-10]. LED lamps are considered both sources and victims of SH. The study in [10] comes to a conclusion that operation failure of LED lamp electronic control units can occur due to the interference between LED lamps and SH distortion in the grid voltage. The interferences in LED driver converters due to the voltage distortion in the SH range are studied in [11] and it is found that, the LED lamp light intensity is affected due to three mechanisms: earlier conduction/later blocking caused

This paragraph of the first footnote will contain the date on which you submitted your paper for review, which is populated by IEEE. This research is funded by Flanders Innovation & Entrepreneurship (VLAIO) and is part of the cSBO project IMPERFECT (HBC.2021.0175). (Corresponding author: Marwa S. Osheba.)

Marwa S. Osheba is with Ghent University, Faculty of Engineering and Architecture, Department of Electromechanical, Systems and Metal Engineering, Research group EnSy/Lemcko, Kortrijk 8500, Belgium, and also with the Department of Electrical Engineering, Faculty of Engineering, Menoufia University, Menoufia 32511, Egypt. (e-mail: Marwa.osheba@ugent.be).

Abdellatif M. Aboutaleb is with Ghent University, Faculty of Engineering and Architecture, Department of Electromechanical, Systems and Metal Engineering, Research group EnSy/Lemcko, Kortrijk 8500, Belgium, and also with the Department of Electrical Engineering, Faculty of Engineering, Menoufia University, Menoufia 32511, Egypt. (e-mail: Abdellatif.aboutaleb@ugent.be).

Jan Desmet is with Ghent University, Faculty of Engineering and Architecture, Department of Electromechanical, Systems and Metal Engineering, Research group EnSy/Lemcko, Kortrijk 8500, Belgium. (e-mail: janj.desmet@ugent.be).

Jos Knockaert is with Ghent University, Faculty of Engineering and Architecture, Department of Electromechanical, Systems and Metal Engineering, Research group EnSy/Lemcko, Kortrijk 8500, Belgium. (e-mail: jos.knockaert@ugent.be).

Color versions of one or more of the figures in this article are available online at http://ieeexplore.ieee.org

by SH voltages, intermittent conduction depending on the SH impedance of the LED driver and reverse-recovery current of the diodes at higher frequency. In [12], it is observed that, LED lamp driver converters interact with the non-synchronized SH voltage components at the point of connection (PoC) with the grid, causing the converter to work as an interharmonic source of emissions.

The components with frequencies that are non-integer multiples of the grid frequency, up to 2 kHz, are defined as interharmonics. The existence of interharmonic components in the background voltage leads to many consequences, such as: distortions, energy losses leading to equipment heating, mechanical system oscillations, acoustic disturbances, and interference with power communication lines [13-15]. Limits to voltage interharmonics are given in [16, 17] up to the second harmonic based on the flicker effect. The interharmonic components can exist in the grid voltage intentionally and non-intentionally. Ripple control systems, typically interharmonics with frequencies between 100 Hz and 3 kHz, are added intentionally to the grid voltage [18]. In [12], it is provided that, interharmonics are generated unintentionally from GCCs due to the existence of non-synchronized SH components found in the grid voltage.

B. Flicker

Despite the low power rating of the majority of the LED lamps, it is crucial to study their aggregate emissions and the effects of their interactions with the background distortions as they are widely used in large numbers in office and residential contexts. One of the consequences that should be clearly studied is the light flicker. Flicker is defined as 'the impression of unsteadiness of visual sensation induced by a light stimulus whose luminance or spectral distribution fluctuates with time' [16, 19]. The flicker has many negative effects on humans. The flicker increases the human observation reaction time. In addition to that, flicker decreases comfort, readiness, ease of maintaining focus and object identification [20] and induces headaches. Based on the bad consequences of the light flicker, many studies have been conducted to address the origin and the effects of flicker in LED lamps. In [21,22], it is concluded that flicker appears in LED lights due to the existence of LF interharmonic components in the grid voltage. The relationship between the flicker frequency and the LF interharmonic frequency is presented in [22]. The conclusion in [23] is that, the deviation of the interharmonic from the nearest harmonics appears in the LED lamp light intensity as flicker. The results in [23] are compatible with the results found in [24]. The study in [24] came to a conclusion that the interharmonic existing in the grid voltage interferes with the GCCs, resulting in additional subharmonics emitted from these GCCs. The relationship between the generated subharmonic frequencies and the interharmonics is the same as found in [23].

C. Research Questions and Motivations

Many studies claim that one of the main interference problems in LED lamps due to the SH existence in the grid is the light flicker [25, 26]. However, the effect of SH distortion in light flicker produced by commercial LED lamps is still vague. As a result, this paper is introduced to give a comprehensive study on the effect of grid distortion in both LF and SH ranges on the light flicker of low power LED lamps. Low power LED lamps are widespread in LV installations [27]. An experimental test setup is implemented, and four scenarios are investigated. The first scenario is done by subjecting the low power LED lamp to a grid distorted with a harmonic component. The second scenario is carried out by exposing the low power LED lamp to an interharmonic distortion in the grid. The third one is carried out to investigate the effect of a SH component with a frequency that is an integer multiple of the grid frequency on the low power LED lamp flickers. The SH component with a frequency that is an integer multiple of the grid frequency is further denoted as SH with integer order. In scenario 4, the effect of a SH component with a frequency that is a non-integer multiple of the grid frequency is observed. The SH component with a frequency that is a non-integer multiple of the grid frequency is called SH with non-integer order in the rest of the paper. It is observed in scenarios 1 and 3 that, no visible light flicker is detected. Visible light flicker is observed for scenarios 2 and 4. The paper explains the phenomena observed in the four scenarios based on the construction of the low power LED lamps. The root causes are analyzed, and the main outcomes are verified through simulation studies in MATLAB/Simulink. The four scenarios are supported by experiments.

The main motivations of this paper can be listed as:

- The SH related EMI interference problems are a hot topic due to the lack of standardization in that range.
- LED lamps are considered one of the most commonly used devices for lighting, which work as both source and victim for the grid distortions in the LF and SH ranges.
- The SH components originate in the grid, both intentionally from power line commutation (PLC) systems and non-intentionally from pulse width modulation (PWM) converters.
- The SH with non-integer order exists in the grid due to the switching frequency deviations of PWM converters due to the impurities in the components and the unavoidable flaws in the design process. Also, the variable frequency drives (VFDs) contribute to polluting the grid with SHs with non-integer order [28].
- The interharmonics exist intentionally from ripple control systems and non-intentionally from GCCs due to the existence of non-synchronized SH components found in the grid voltage.

The contributions of this paper can be listed as:

- Proving that the harmonics, as well as the SH with integer order distortion in the grid, have no effect on the visible light flicker for low power LED lamps.
- Observing the effect of the interharmonic distortion in the grid on the low power LED lamps and clarifying the inverse relationship between the visible light flicker and the interharmonic frequency.
- Explanations for the effect of the existence of SH with non-integer order on the LED lamp flicker.

The rest of the paper is organized as follows. The experimental studies and observations are given in section II. Section III provides discussions and explanations on the main observations of section II. The simulation studies are presented in section IV.

II. Photometric flicker assessment criteria

A. *Brief Review*

Several techniques are used to evaluate the optical flicker, such as flicker index [29]and percent flicker specified by IEEE 1789:2015 [30]. As explained in [31, 32], those methods have various weaknesses, for instance, not being sensitive to the frequency and appearing to have discontinuity at 90 Hz. In addition, the Light Research Center (LRC) extends the measuring techniques, of the intentional light waveform, called LRC flicker meter [33]. In the LRC flicker meter, the measured light waveform from the light sensor is analyzed with the Fast Fourier Transform (FFT), and the resulting components are weighed in order to take the human eye sensitivity into consideration. However, a significant drawback of this method is that it does not account for the human sensitivity to flicker in the 100-200 Hz range.

B. *Compact Flicker Degree Definition*

The evaluation approach in the current research is the Compact Flicker Degree (CFD) method [32,33]. The degree of the flicker is estimated by converting the light intensity waveform into an electrical voltage then resolving it into Fourier components, then taking the root mean square (RMS) of the weighted frequency. The main profit of the CFD is taking into consideration the frequencies up to 2000 Hz rather than stopping around 100 Hz as LRC flicker meter technique.

C. *Color Region Clarification*

The degree of the flicker can be assessed in five different regions: imperceptible, acceptable, moderate, strongly affected and extremely affected. Every area is depicted using a distinct color, as illustrated in Figure 1. The deep green region, ‘imperceptible’, is in the CFD percent range of 1% to 12%; it is almost undetectable to humans. When the flicker degree is from 12% to 25%, it is in the light-green region, which is ‘acceptable’ and recommended for general use but not recommended in offices. In the ‘moderate’ region, the flicker degree ranges are between 25% and 50%, this is the yellow region. This is possibly perceptible, so it is much less appropriate for working places. Flickering between 50% and 75%, colored as the orange region, is known as ‘strongly affected’[33]. This level has a high influence, so long-term exposure causes discomfort and headaches. The ‘extremely affected’ region has a flickering degree above 75% and is in the red region, it has extreme influence. Regions four and five are hazardous for work and must be avoided [21].

D. *CFD calculations*

In this approach the light waveform is taken into consideration then converted to a voltage signal. This waveform is analyzed in a series of processes, whereafter the CFD value is calculated:

$$CFD_{FB} = \sqrt{\sum_{K=1}^{N-1}(100\ \frac{A_K}{A_0} * M_{W(f)})^2} \qquad (1)$$

Here A_0 and A_K are the DC components of the signal and the amplitude of each harmonic, respectively. $M_{W(f)}$ represents the weight function that specifies a specific value for each frequency (Fig. 2), taking into consideration the eye sensitivity and the flicker unconsciously sensed in the peripheral field of vision. Furthermore, fig. 2 illustrates the corresponding equivalent value for each frequency, ensuring a comprehensive consideration of these factors. Consequently, higher weights are clearly allocated to frequencies that are detectable by the human eye.

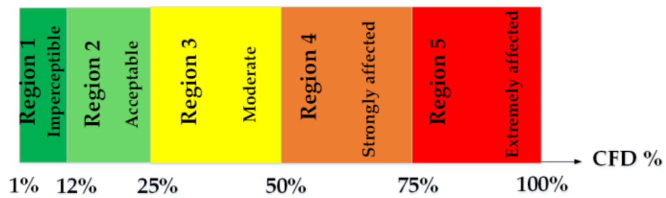

Fig 1. CFD severity classification.

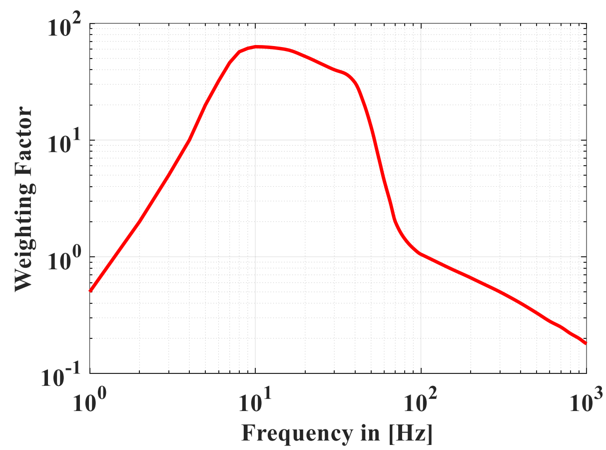

Fig 2. Weight function CFD.

III. Experimental Test setup description

The experimental setup is shown in figure 3. It consists of an enclosure that contains a commercial PEL00530 LED lamp and a light sensor. The box can be fully closed to have no influence from external lights. The SEEED STUDIO 314990740 light sensor is used to convert the light intensity into a voltage signal that can be captured using an oscilloscope. There are two different power sources for supplying the LED lamp. The first source is the PCR2000 programmable voltage source, whose output voltage can be shaped and controlled up to 1000 Hz. The second source is the IMU-MGS with the differential mode voltage/current module, which is used mainly for performing the immunity test defined in [32]. The first power supply is used to generate interharmonics between 50 Hz and 1 kHz. The second power supply is used to add SH components to the grid voltage that is applied across the LED lamps.

To measure the lamp current, a 100 MHz bandwidth TCP A300 AC-DC current probe is used. The voltage of PoC is measured with a 25 MHz Pico differential voltage probe. The data are captured with a 20 MHz, 4000 series PicoScope. The data is plotted and analyzed using the MATLAB® software environment.

Four experimental scenarios are performed; the first and the second ones are done by supplying the LED lamp from the PCR2000 programmable voltage source. In the first two studies, the effects of LF harmonics and interharmonics distortion on the grid voltage on the LED lamp Flicker are studied. The third and fourth ones are done to study the effect of the HF distortions in SH range on the grid voltage on the LED lamp flickers. The CFD method is used for the assessment of the flicker. As this method depends on the FFT analysis of the light intensity for the assessment of the flicker degree, the FFT analysis for all cases is provided. The SH components are added to the grid by the means of the IMU-MGS with the differential mode voltage/current module.

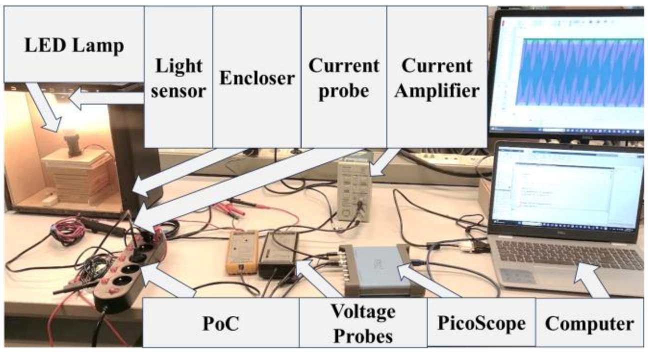

(a)

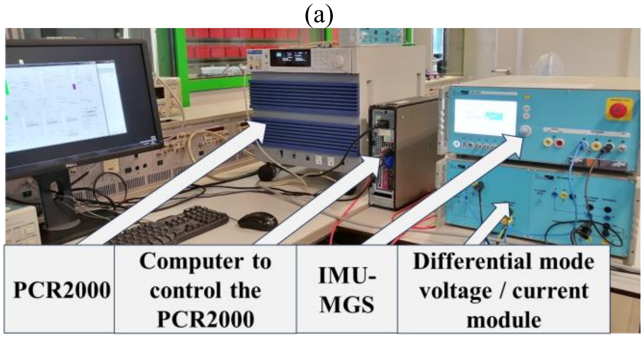

(b)

Fig 3. Experimental setup. (a) LED lamp measurements setup. (b) Power sources used to energize the LED lamps.

IV. Results and Observations

In this section, the measurement results and the related observations are discussed. The measurements are performed for four scenarios. The first and the second scenarios cover the effect of harmonic and interharmonic LF distortion in the grid voltage on the LED light intensity. The effects of the grid distortion with SH components that are of integer and non-integer orders represent scenarios 3 and 4.

Before beginning the four scenarios, the low power LED lamp is just connected to the grid as a reference scenario. The time and frequency domains of the LED lamp terminal voltage and current are as shown in fig. 4. It is obvious that, the LED lamp injects many LF harmonics, as there is no obligation for the manufacturer to follow the power quality regulations [section 7 of [35])]. In addition to that, background LF distortion is detected in the grid voltage, which is in the limit defined in IEC 61000-3-2 [36]. No subharmonic components are detected in the light intensity, which is confirmed by the light intensity measurements in both time and frequency domains (fig. 5).

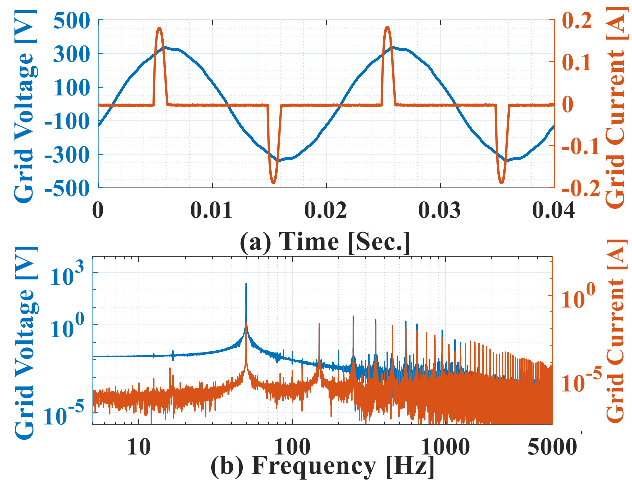

Fig. 4. Voltage and the current measured at the LED lamp terminals with no background distortion. (a) Data in time domain. (b) Data in frequency domain.

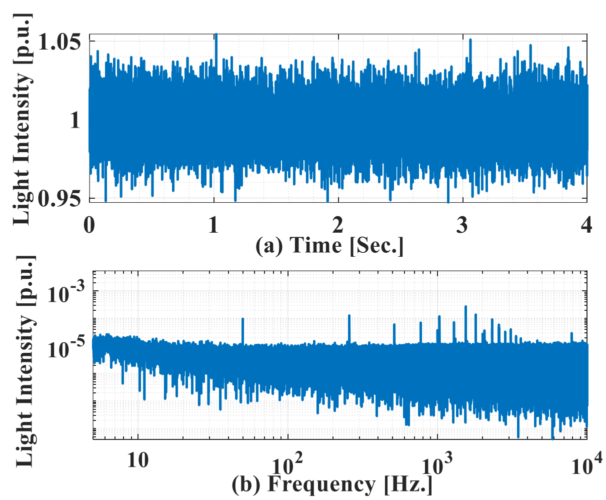

Fig. 5. Voltage and the current measured at the LED lamp terminals with no background distortion. (a) Data in time domain. (b) Data in frequency domain.

A. Scenario 1: LED lamp subjected to a harmonic.

In this scenario, the effect of the LF harmonic is analyzed. This study is performed by adding 150 Hz voltage distortion with a magnitude of 5% of the fundamental voltage component, which is equal to the limit provided in EN 50160 [35]. The measured data of the terminal voltage and current of the LED lamp is as shown in fig. 6. It is noticeable that there is high frequency distortion appearing around 10 kHz due to the switching behavior of the PCR2000. However, it has no impact on the results of this and the following scenarios. The negligible effect of SH distortions on the LED lamp flickers is discussed in scenarios 3 and 4. Fig. 7 shows the corresponding light intensity in both time and frequency domains. It is observed that, no component is detected in the light intensity below 50 Hz. So, it can be concluded that, the LF distortions are not liable for any visible light flickers appearing in low power LED lamps.

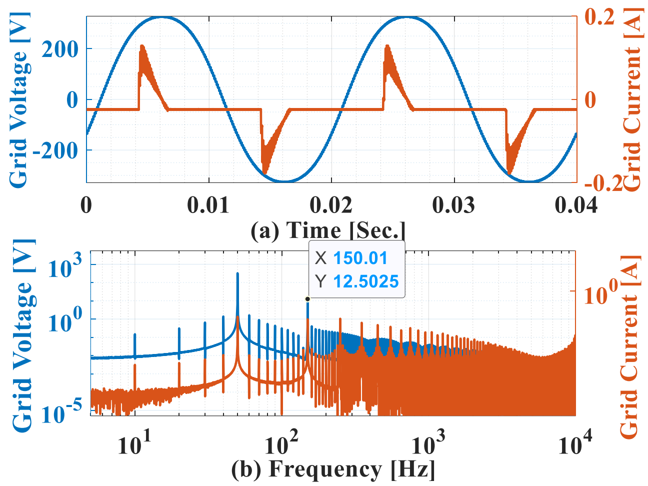

Fig. 6. Voltage and current measured at the LED lamp terminals at 150 Hz distortion . (a) Data in time domain. (b) Data in frequency domain.

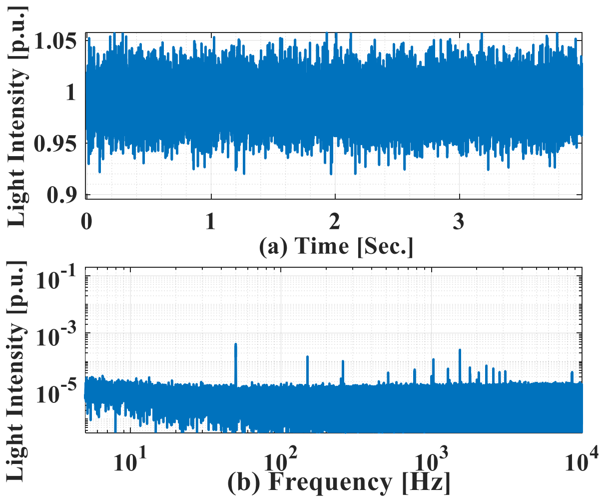

Fig. 7. Voltage and current measured at the LED lamp terminals at 150 Hz distortion. (a) Data in time domain. (b) Data in frequency domain.

B. Scenario 2: LED lamp subjected to an interharmonic.

The interharmonic distortion effect in the LF range in the grid voltage on the light flicker of the LED lamp is studied in scenario 2. Two studies are done in this scenario. The first and second studies are performed by adding 60 Hz and 260 Hz voltage components, respectively, with the same amplitudes to the grid voltage at the LED lamp terminals.

Study 1 results are as shown in figures 8 and 9. Fig. 8 is for the LED lamp terminal voltages and currents. While fig. 9 shows the light intensity of the LED lamp. Figures 10 and 11 represent study 2 of scenario 2. The LED lamp terminal voltage and current are shown in fig. 10. The light intensity of the LED is presented in fig. 11. In both studies, a visible light flicker at 10 Hz is spotted in the frequency domain of the LED light intensity. However, the 10 Hz flicker for the 60 Hz distortion is higher than its counterpart for the 260 Hz distortion. This result is compatible with the studies in [21] and [22], which conclude that, as the interharmonic frequency increases, the light flicker decreases, without further explanation of this phenomenon. This phenomenon is thoroughly addressed in the following section. Fig. 12 illustrates the impact of increasing the interharmonic frequencies on the flicker degree.

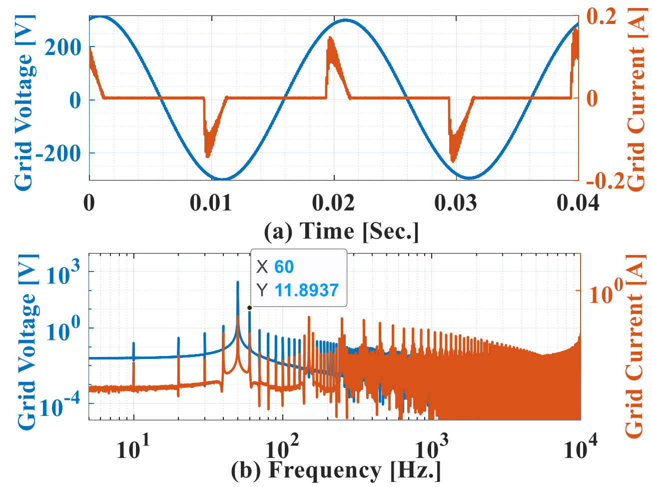

Fig. 8. Voltage and current measured at the LED lamp terminals at 60 Hz distortion. (a) Data in time domain. (b) Data in frequency domain.

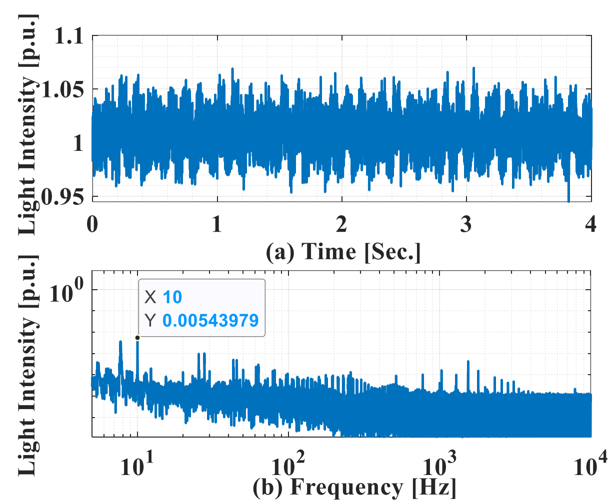

Fig. 9. Measured light intensity of the LED lamp at 60 Hz distortion. (a) Data in time domain. (b) Data in frequency domain.

C. Scenario's 3 and 4: LED lamp subjected to an SH with integer order and non-integer order

The LED lamp light flicker under a grid distorted with a SH with integer order is now investigated. A 5 kHz SH is added to the grid voltage at the LED lamp terminals. However, although the measuring devices are fully compliant with the standard IEC61000-4-19, a perfect harmonic frequency cannot be reached. This result in 5.01615 kHz, which is a SH component with non-integer multiple. It means scenario 3 cannot be formed at a perfect harmonic frequency. No flicker components are observed in the light intensity measured data in fig. 14.

Other interharmonic frequencies above 2 kHz are tested. A 4.16 kHz voltage component is supplied to the LED lamp

terminal voltage. However, as mentioned previously, the $4.16\ kHz$ appears as $4.17348\ kHz$. This is no problem in this scenario as the $4.17348\ kHz$ voltage component is also considered as a SH with non-integer multiple.
The terminal voltage and current of the LED lamp are as illustrated in fig. 15, while fig. 16 shows the corresponding light intensity. No visible light flicker is observed in the frequency domain data of the light intensity in fig. 16.
Fig. 17 shows the effect of supraharmonics components on the flicker of LED lamp at different frequencies. It's obvious that, the degree of the flicker at the measured frequencies is in the green region.

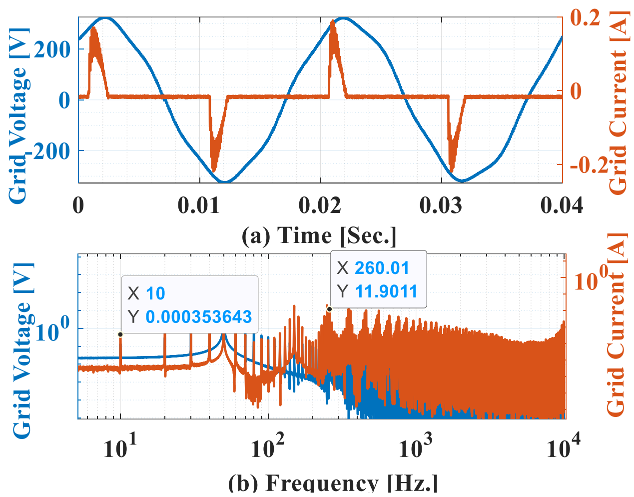

Fig. 10. Voltage and current measured at the LED lamp terminals at 260 Hz distortion. (a) Data in time domain. (b) Data in frequency domain.

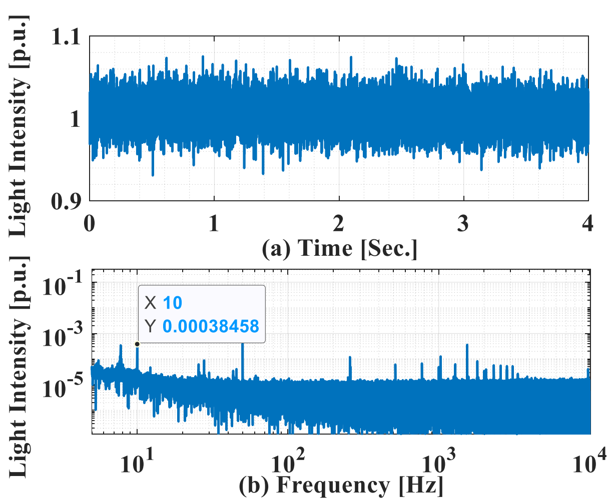

Fig. 11. Measured light intensity of the LED lamp at 260 Hz distortion. (a) Data in time domain. (b) Data in frequency domain.

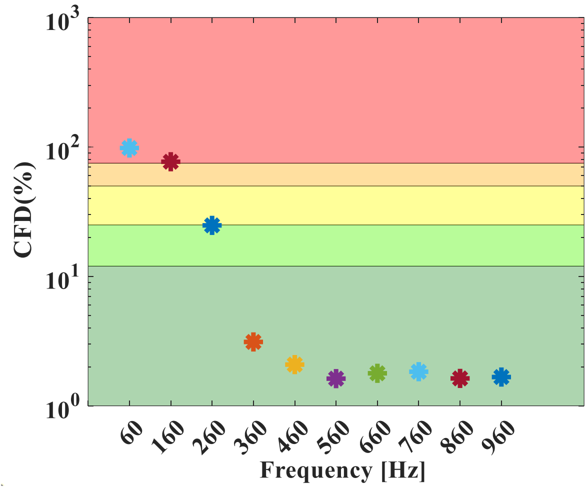

Fig 12. CFD results for the influence of LF interharmonics experimentally

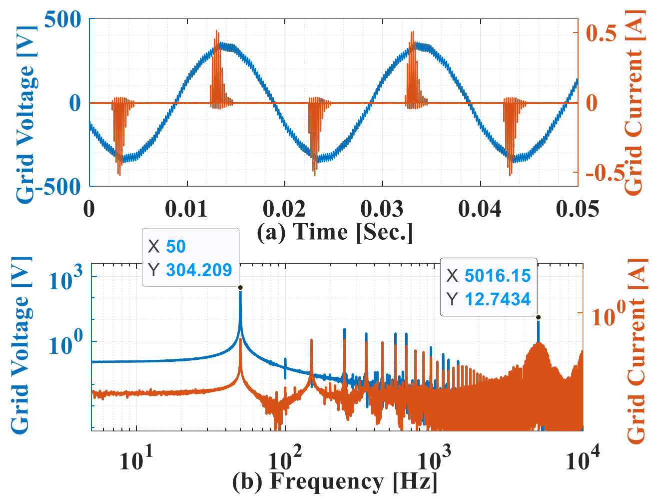

Fig. 13. Voltage and current measured at the LED lamp terminals at 5016 Hz distortion. (a) Data in time domain. (b) Data in frequency domain.

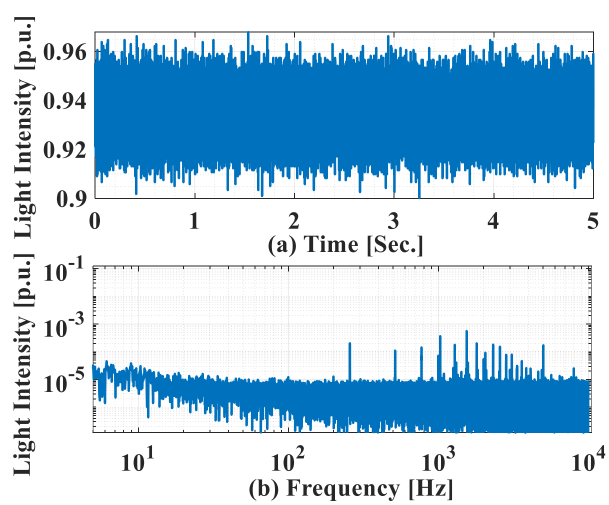

Fig. 14. Measured light intensity of the LED lamp at 5016 Hz distortion. (a) Data in time domain. (b) Data in frequency domain.

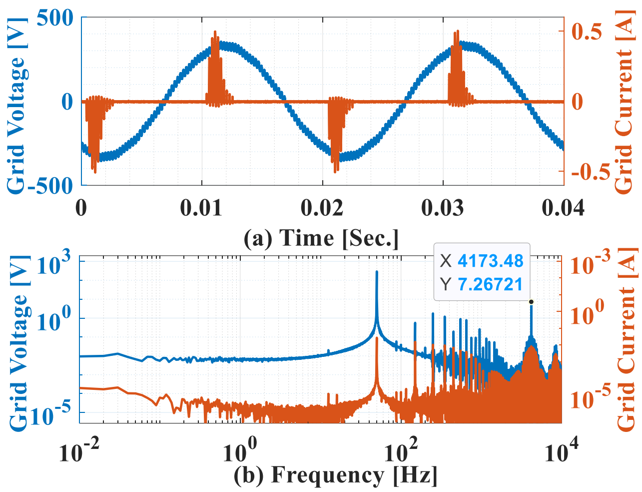

Fig. 15. Voltage and current measured at the LED lamp terminals at 4173 Hz distortion. (a) Data in time domain. (b) Data in frequency domain.

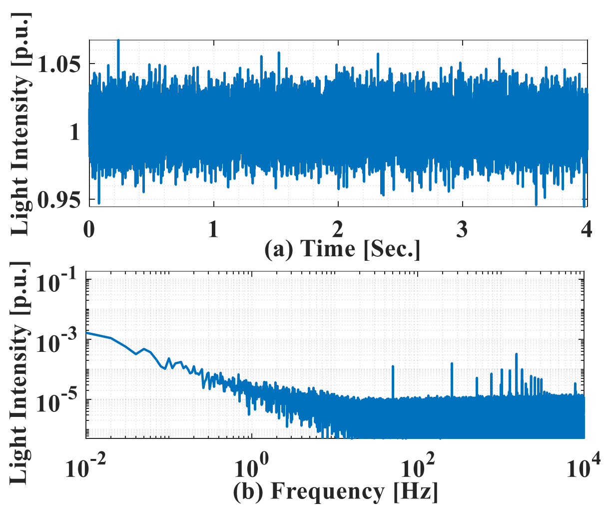

Fig. 16. Measured light intensity of the LED lamp at 4173 Hz distortion. (a) Data in time domain. (b) Data in frequency domain.

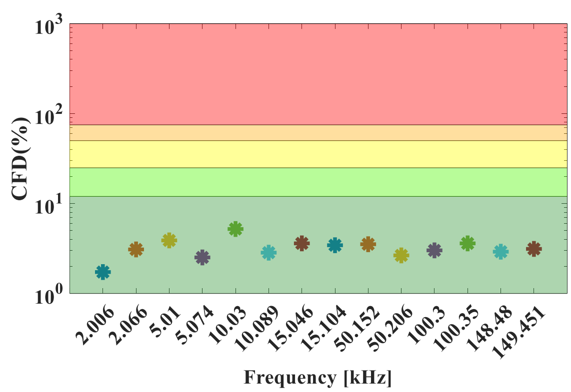

Fig. 17. Influence of measured SH components on LED flicker

V. Discussions and Observations

In this section, the results and observations of the measurements of section II are discussed. This section is divided into three subsections. In the first subsection, the different types of LED lamp drivers are discussed, showing why the LED lamp used in the measurements are chosen for these tests. In the second and third subsections, explanations of the phenomenon found in the measurements are provided.

A. LED lamp constructions

LEDs are semiconductor devices that normally require a DC current source to operate. However, the public LV grid provides AC power. In order to match the requirements of the LEDs from the LV network, 8 approaches can be applied [27]. These approaches are illustrated in fig. 18.

Type 1 is the simplest and it is called capacitive divider circuit. In this type, a diode bridge rectifier (DBR) is used to convert the AC power into DC power. Two capacitors are used; the first capacitor is connected in series with the grid at the AC side of the DBR, and the second capacitor is connected at the DC side of the DBR. These two capacitors form a voltage divider to reduce the supply voltage magnitude. Additionally, a resistor is connected in series with the LEDs to limit the LEDs current. In many commercial LEDs, the AC side capacitor is replaced by a resistor. This type is the most commonly used one in the low power applications due to its simplicity. In this type, below 5 w, the LF harmonic limitations can be not applied (section 7 of [35]). As a result, this type is installed with large numbers in LV installations. Consequently, this type of LED lamp is used to perform the tests.

The rest of the LED types shown in fig. 18 are out of the scope of the paper. Further details about these topologies are documented in [27], [38-40].

B. Rectifier effect

If the grid contains an injected harmonic current originated from the background distortion as in fig 19, the harmonic current is transferred to the DC side of the DBR. The DBR function that affects the harmonic current transfer from the AC to the DC side can be represented as [41, 42]:

$$u_{DBR}(t) = \sum_{k=2n+1}^{\infty} \frac{2}{k\pi} \sin\left(\frac{k\pi}{2}\right) \cos\left(2\pi \cdot k f_g \cdot t\right) \tag{2}$$

Here, u_{DBR} is the DBR function, f_g is the LV grid frequency and $n \in N_0$. Let the current harmonic component be represented by the following equation:

$$i_h = I_h \cdot \cos(2\pi f_h t) \tag{3}$$

Here, i_h is the instantaneous value of the current harmonic component, I_h is the amplitude of the current harmonic component, and f_h is the harmonic frequency. The current harmonic component at the DC side of the DBR can be obtained by multiplying (2) by (3). Equation (4) describes the DBR DC side current.

$$i_{h-DC} = \sum_{k=2n+1}^{\infty} \left(\frac{I_h}{k\pi} \sin\left(\frac{k\pi}{2}\right)\right).\left(\cos\left(2\pi\left(f_h - kf_g\right)t\right) + \cos\left(2\pi\left(f_h + kf_g\right)t\right)\right) \quad (4)$$

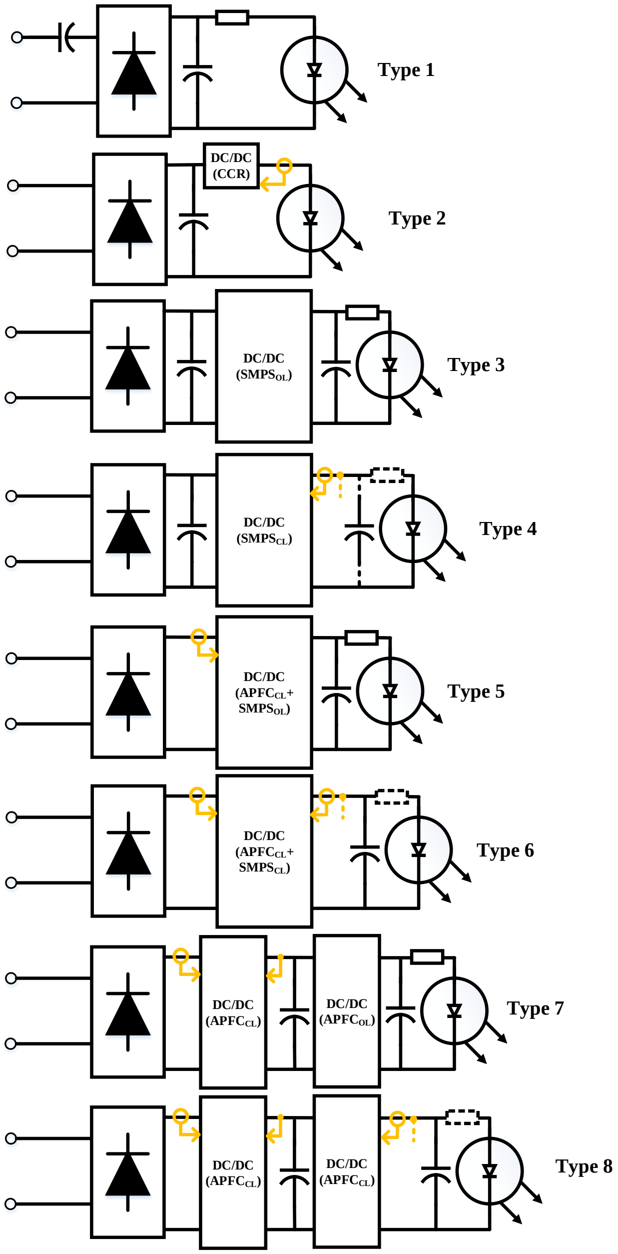

Fig. 18. Different topologies of LED drivers.

It can be concluded from equation (4) that the DBR resolves the AC side harmonic into an infinite number of harmonics which appear as a sideband harmonic around the harmonic frequency as shown in fig. 19 (a). Consequently, at a specific k, there is a DC side harmonic component with a frequency located at the visible flicker range. This occurs when $f_h - kf_g$ lies in the visible flicker region. Consequently, as the harmonic frequency increases, the value of k increases. This, in turn, reduces the value of $\frac{I_h}{k\pi}\sin\left(\frac{k\pi}{2}\right)$ at the visible frequency as the harmonic frequency increases. The current component at the visible flicker region is divided between the DC link capacitor and the LEDs equivalent branch resistance as:

$$\boldsymbol{I}_{h-LED-flick} = \boldsymbol{I}_{h-DC-flick} \times \frac{X_{C_{dc-flick}}}{X_{C_{dc-flick}} + R_{LED}} \quad (5)$$

Here, $\boldsymbol{I}_{h-LED-flick}$ and $\boldsymbol{I}_{h-DC-flick}$ are the phasor representations of the DC-side harmonic current component through the LEDs and through the DC-Link capacitor at the visible frequency region respectively, $\boldsymbol{X}_{C_{dc-flick}}$ is the phasor representation of the DC-link capacitive reactance at the frequency of $\boldsymbol{I}_{h-LED-flick}$ and R_{LED} is the LEDs branch equivalent resistance. Then, the LEDs convert $\boldsymbol{I}_{h-LED-flick}$ into light intensity as [43]:

$$I_V = M \cdot \boldsymbol{I}_{h-LED-flick} \quad (6)$$

Here I_V is the light intensity of the LEDs at the visible frequency region, M is the conversion constant from current to light intensity. The relationship between I_V and $\boldsymbol{I}_{h-LED-flick}$ is considered to be linear for simplicity.

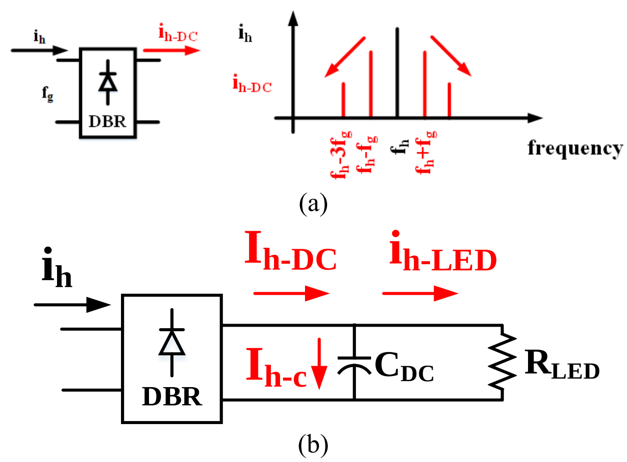

Fig. 19. DBR effect

Now, if k is an integer value as the ones done for scenarios 1 and 3 for harmonic and SH ranges, the lower frequency of I_V would be 50 Hz. For example, If the current harmonic in the grid occurs at 250 Hz, then k is 3 at 100 Hz. As a result, the flicker occurs at 100 Hz which cannot be detected by the human eye. On the other hand, for scenarios 2 and 4, k becomes a non-integer value. For example, if the grid contains a 160 Hz component, the only value of k that gives a frequency in the visible region is 3. As a result, I_V appears with a 10 Hz component which can be detected by the human eye. It is worth noting that, from (4), with the increase of interharmonic frequencies, k increases and the amplitude of the 10 Hz component at I_V decreases. Consequently, the main difference between scenario 2 and 4, is that the frequencies of interharmonic components are much lower than the frequencies of SH with non-integer orders. Therefore, k values are much higher in scenario 4 than its values in scenario 2. As a result, I_V effect can be negligible for scenario 4.

VI. Simulation verifications

To verify and emphasize the experimental test results observation, discussions, and explanations provided, a model of a commercial LED lamp that is used in the experimental setup, GP 4.3 watt, is decapsulated and a MATLAB/Simulink LED lamp is developed. The construction of the LED lamp, after exploring it, is found in the schematic in fig. 20 which is compatible with the type 1 construction discussed in subsection IV.A.

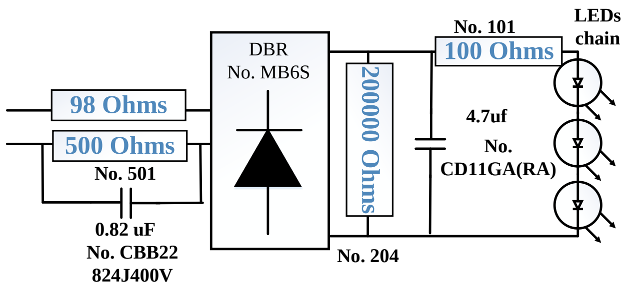

Fig. 20. a 4.3 LED lamp construction used for the simulation study

The reference scenario of the experimental study is performed in simulation by just connecting a pure sinusoidal voltage to the LED lamp model. The simulated results of the terminal voltages and currents are shown in fig. 21, whereas the related light intensity is shown in fig. 22. From the simulated results, the LED lamp emits multiple LF emissions which, in turn, pollute the terminal LED lamp voltage. However, no additional components are observed in the light intensity results in fig. 18.

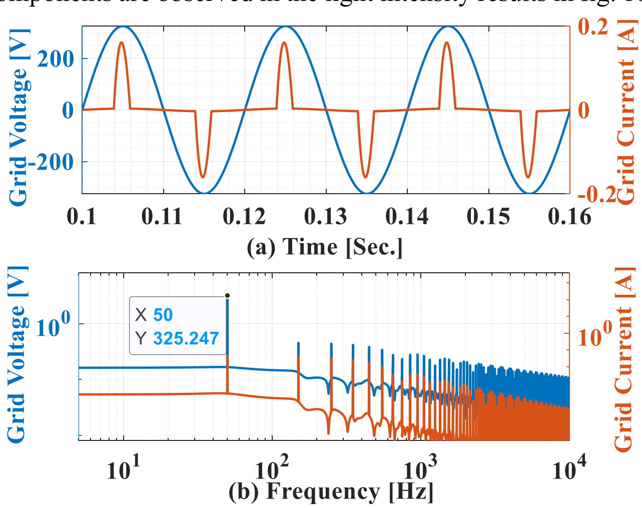

Fig. 21. Simulated voltage and current at the LED lamp terminals with no background distortion. (a) Data in time domain. (b) Data in frequency domain.

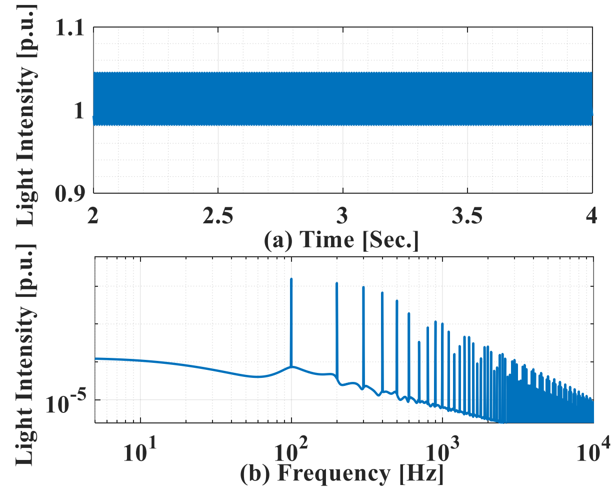

Fig. 22. Simulated light intensity of the LED lamp at no background distortion. (a) Data in time domain. (b) Data in frequency domain.

A. Scenario 1: LED lamp subjected to a harmonic.

A 150 Hz distortion of scenario 1 of the experimental study is done in simulation. The simulated results of the terminal voltage and current are as shown in fig. 23. The resultant light intensity simulation results in both time and frequency domains are illustrated in fig. 24. As clarified in section IV that, the 150 Hz component is dissolved in the DC side of the rectifier into infinite components following equation (4). One of these components appears at 100 Hz, which is not a visible flicker.

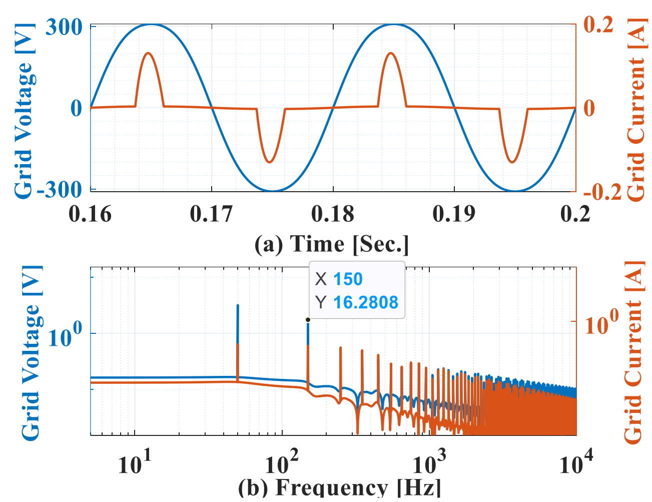

Fig. 23. Simulated voltage and the current calculated at the LED lamp terminals at 150 Hz distortion . (a) Data in time domain. (b) Data in frequency domain.

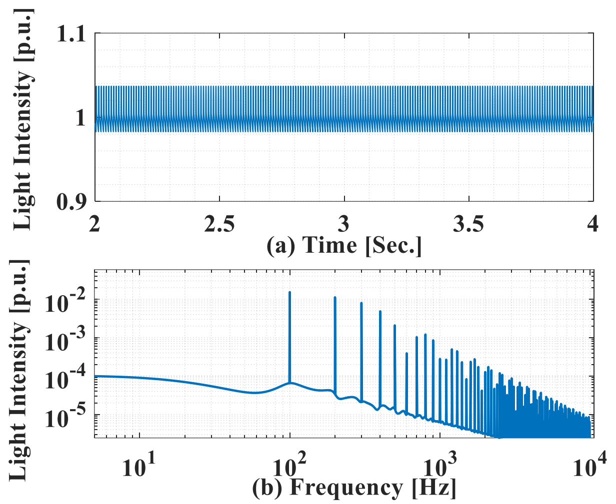

Fig. 24. Simulated light intensity of the LED lamp at 150 Hz distortion. (a) Data in time domain. (b) Data in frequency domain.

B. Scenario 2: LED lamp subjected to an interharmonic.

Scenario 2 of the experimental study is simulated by adding the same two interharmonics at 60 Hz and 260 Hz with the same magnitudes, forming study 1 and study 2, respectively. The simulation results of study 1 are shown in fig. 25 for the terminal voltages and currents and in fig. 26 for the light intensity. The study 2 results are presented in fig. 27 for the terminal voltage and current, while the simulation results of the light intensity of study 2 are given in fig. 28. For both studies, the light flicker at 10 Hz appears. However, the flicker at 10 Hz in study 2 is less than the one of study 1. This is because the order of the 10 Hz of the DC side reflection of the interharmonic components, as $k = 1$ and $k = 3$ for study 1 and 2 respectively. This in turn, based on equation (4), leads to having a lower 10 Hz component in the DC side current of the DBR in study 2 than study 1.

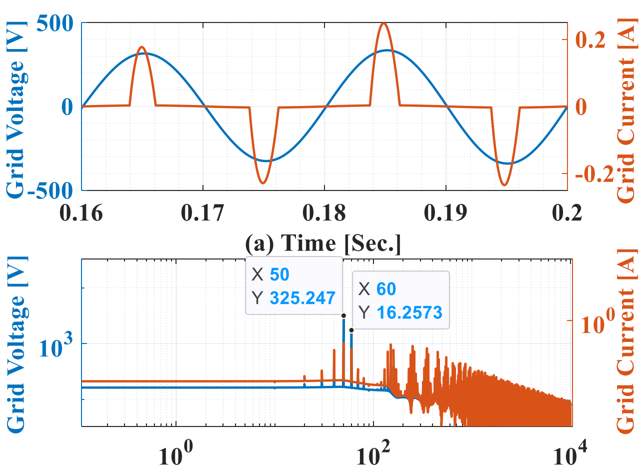

Fig. 25. Simulated voltage and current calculated at the LED lamp terminals at 60 Hz distortion. (a) Data in time domain. (b) Data in frequency domain.

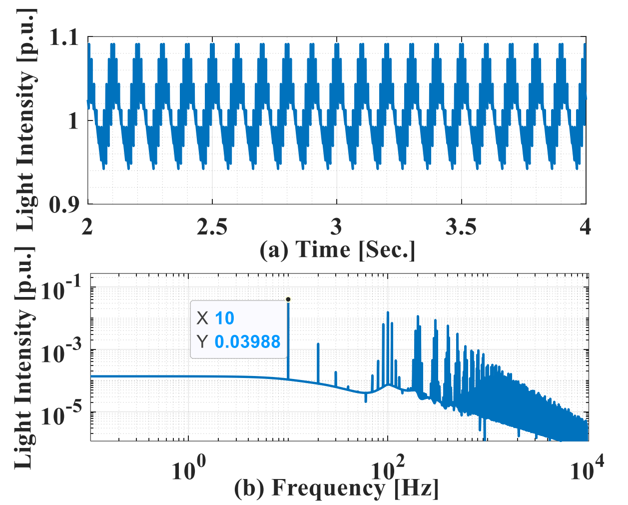

Fig. 26. Simulated light intensity of the LED lamp at 60 Hz distortion. (a) Data in time domain. (b) Data in frequency domain.

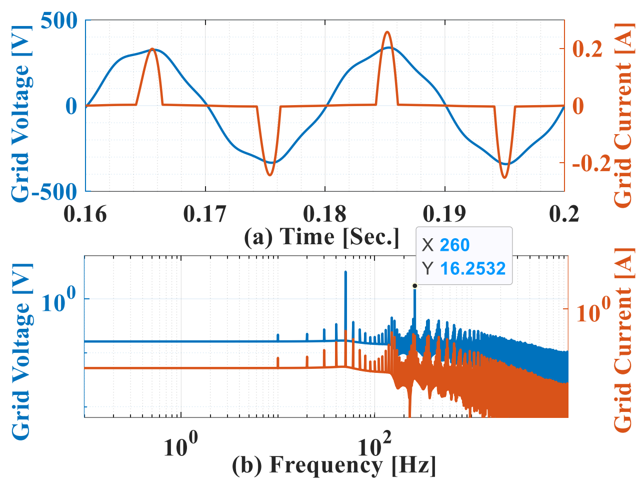

Fig. 27. Simulated voltage and current calculated at the LED lamp terminals at 260 Hz distortion. (a) Data in time domain. (b) Data in frequency domain.

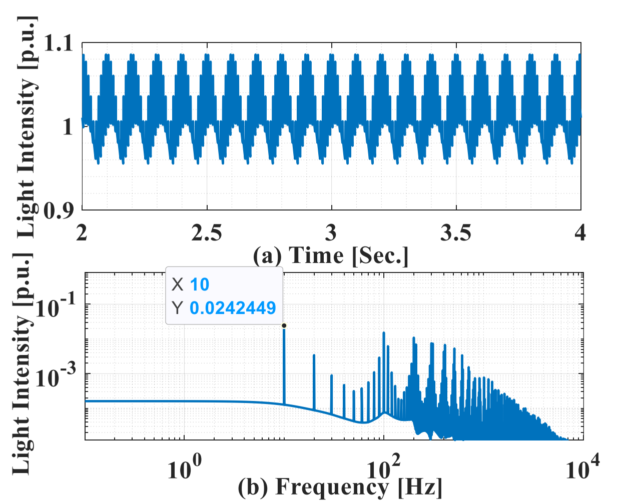

Fig. 28. Simulated light intensity of the LED lamp at 260 Hz distortion. (a) Data in time domain. (b) Data in frequency domain.

The degree of the flicker is assessed by the CFD method for the LF harmonic and interharmonic components from 160 Hz up to 1160 Hz (fig. 29). It is found that the degree of flicker decreases with the increasing frequency of the LF components. The flicker increases when the interharmonic comes closer to a harmonic frequency but drops to a minimum at the harmonic frequency itself.

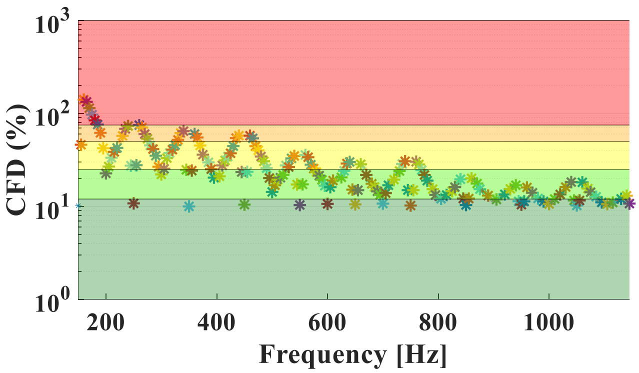

Fig. 29. CFD results for the influence of LF interharmonics

C. Scenario 3: LED lamp subjected to an SH with integer order

In simulation, scenario 3 can be performed well, which solves the problem previously mentioned in the experimental study. In this study an exact 5 kHz voltage component is added at the LED lamp terminals in series with the grid. The simulation results of this scenario are shown in fig. 30 for the terminal voltage and currents of the LED lamp model and in fig. 31 for the resultant LED lamp light intensity. It is clear that, no visible flicker below 50 Hz is detected. This can be explained from equation 4. The 5 kHz component is dissolved into an infinite number of components at the DC terminal. The components of the 5 kHz in the LF range are neglected due to the high value of k, which is enough to neglect its effect.

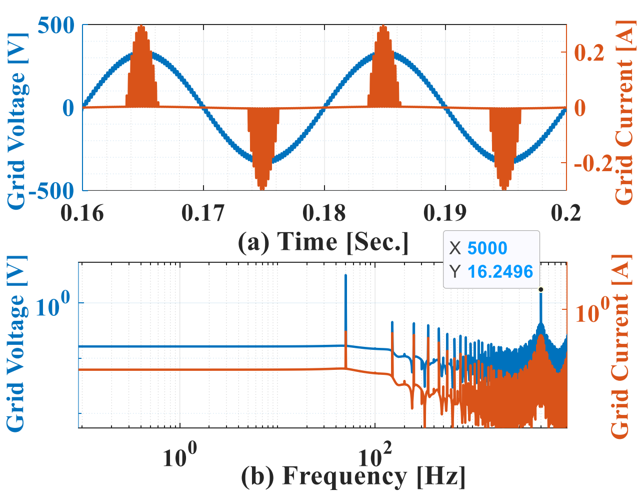

Fig. 30. Simulated voltage and current calculated at the LED lamp terminals at 5 kHz distortion. (a) Data in time domain. (b) Data in frequency domain.

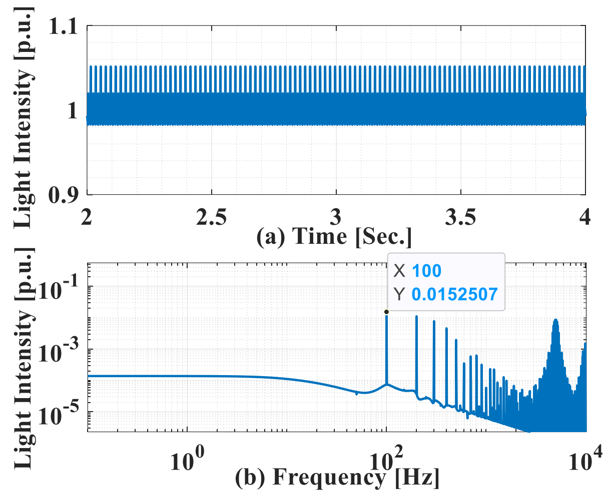

Fig. 31. Simulated light intensity of the LED lamp at 5 kHz distortion. (a) Data in time domain. (b) Data in frequency domain.

D. Scenario 4: LED lamp subjected to an SH with non-integer order

Scenario 4 of the experimental study is performed in simulation by adding a SH component with non-integer multiple at 4160 Hz to the grid voltage at the LED lamp terminals. The time and frequency domain results of LED lamp terminal voltage and current are shown in fig. 32. The generated light intensity simulation data in time and frequency domains are given in fig. 33. It is clear that, no visible light flicker is observed in the frequency spectra of the light intensity. This can be explained as follows. The SH at 4160 Hz at the AC side of the LED lamp DBR is as divided into infinite components in the DC side of the DBR with frequencies $4160 \pm k \cdot 50$ as concluded in equation (4) with a reverse relationship between their amplitudes and the value of k. Consequently, a 10 Hz component must appear on the DC side current of the DBR. However, k is equal to 83 for that component. As a result, the 10 Hz component appears with a negligible value. This negligible 10 Hz component is then divided between the DC-link capacitor and the LEDs branch. Which leads to a negligible visible flicker in the LED light intensity.

Fig 34 illustrates the effect of SHs components with various frequencies on the flicker degree. It is clear from the figure that SH components have no significant effect on the flicker degree.

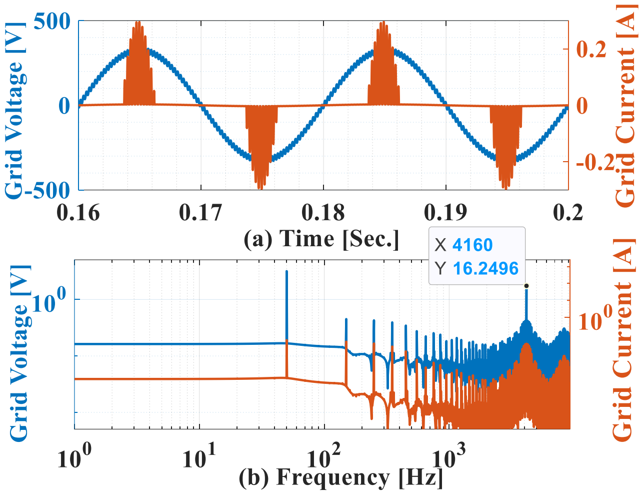

Fig. 32. Simulated voltage and current calculated at the LED lamp terminals at 4173 Hz distortion. (a) Data in time domain. (b) Data in frequency domain.

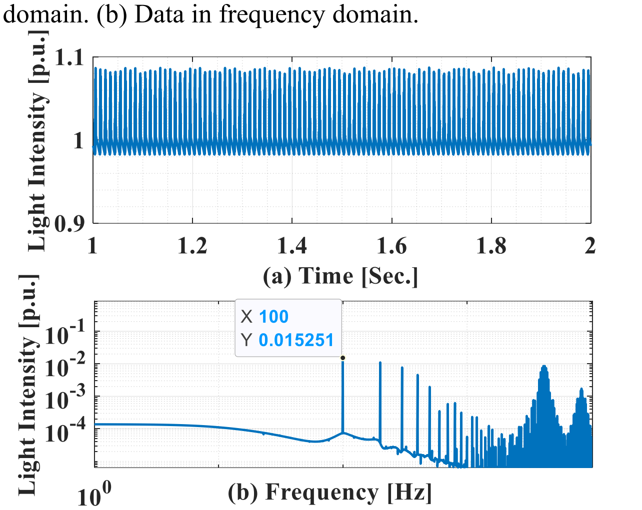

Fig. 33. Simulated Light intensity of the LED lamp at 4173 Hz distortion. (a) Data in time domain. (b) Data in frequency domain.

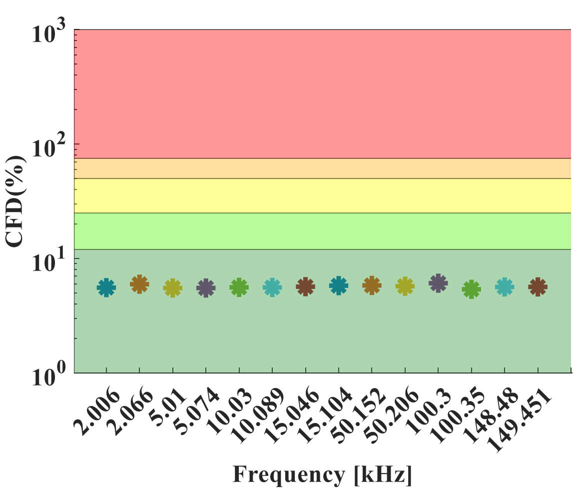

Fig. 34 Influence of SH components on LED flicker

VII. Conclusion and Future Work

In this paper, an assessment of the light flicker produced from low power LED lamps has been presented under grid voltage distortion conditions in both LF and SH ranges. Four scenarios have been performed experimentally. The first and the second one have been done for a grid distorted by harmonic and interharmonic voltage components, respectively. A LV grid with SH distortion with integer and non-integer multiples has represented the third and fourth case studies. It can be concluded from the four scenarios that visible flicker appears clearly in case study 2 with LF interharmonics. No light flicker is detected for case studies 1 and 3 with harmonic distortion and negligible flicker occurs in scenario 4 with high frequency interharmonics. Mathematical analysis has been presented to explain the reasons behind the observed phenomenon. A MATLAB/Simulink model of a commercial low power LED lamp has been built to verify experimental observations and mathematical explanations.

This work can be extended in the future to include the following:

- Evaluating the effects of the four types of distortions on the light flicker produced from other types of the LED lamp drivers shown in fig 18.
- Performing a comparative study for the LED lamp drivers that contain power electronic converters (types 3-8 in fig. 18) to differentiate among their emissions to the grid, their interferences with the background distortions and the effect of their switching nature on the light flicker.

References

[1] J. Meyer *et al*., "Future work on harmonics - some expert opinions Part II - supraharmonics, standards and measurements," *2014 16th International Conference on Harmonics and Quality of Power (ICHQP)*, Bucharest, Romania, 2014, pp. 909-913, doi: 10.1109/ICHQP.2014.6842871.

[2] S. T. Y. Alfalahi *et al*., "Supraharmonics in Power Grid: Identification, Standards, and Measurement Techniques," in *IEEE Access*, vol. 9, pp. 103677-103690, 2021, doi: 10.1109/ACCESS.2021.3099013.

[3] A. M. Aboutaleb, J. Desmet, and Jos Knockaert, "Impact of Grid-Connected Inverter Parameters on the Supraharmonic Emissions in Distributed Power Generation Systems," Machines, vol. 11, no. 11, pp. 1014–1014, Nov. 2023, doi: https://doi.org/10.3390/machines11111014.

[4] A. M. Aboutaleb, J. Desmet and J. Knockaert, "A Novel Active Power Filter for Supraharmonic Emissions of Single Phase Grid-Connected Inverters," in IEEE Transactions on Power Electronics, vol. 40, no. 6, pp. 8109-8124, June 2025, doi: 10.1109/TPEL.2025.3539024

[5] L. Sandrolini and A. Mariscotti, "Waveform and Spectral Characteristics of Supraharmonic Unsymmetrical Conducted EMI of Switched-Mode Power Supplies," Electronics, vol. 11, no. 4, p. 591, Feb. 2022, doi: https://doi.org/10.3390/electronics11040591.

[6] M. S. Osheba, A. E. Lashine, and A. S. Mansour, "Design, implementation and performance evaluation of multi-function boost converter," *Scientific Reports*, vol. 13, no. 1, Mar. 2023, doi: 10.1038/s41598-023-31293-5.

[7] T. Slangen, T. van Wijk, V. Ćuk, and S. Cobben, "The Propagation and Interaction of Supraharmonics from Electric Vehicle Chargers in a Low-Voltage Grid," Energies, vol. 13, no. 15, p. 3865, Jul. 2020, doi: https://doi.org/10.3390/en13153865.

[8] Á. Espín-Delgado, T. Busatto, V. Ravindran, S. K. Rönnberg and J. Meyer, "Evaluation of Supraharmonic Propagation in LV Networks Based on the Impedance Changes Created by Household Devices," 2020 IEEE PES Innovative Smart Grid Technologies Europe (ISGT-Europe), The Hague, Netherlands, 2020, pp. 754-758, doi: 10.1109/ISGT-Europe47291.2020.9248928.

[9] A. J. Collin, J. Meyer, P. Davari, J. Drapela, G. W. Chang and R. Langella, "Modeling the Unintentional Emissions of Single-Phase Power Electronic

Converters for Distortion Studies in the 2-150 kHz Range," in *IEEE Transactions on Power Delivery*, vol. 39, no. 6, pp. 3126-3138, Dec. 2024, doi: 10.1109/TPWRD.2024.3453493.

[10] L. M. Lorenzo-Peñaloza, A. Medina-Rios, J. C. Godinez-Delgado and R. Cisneros-Magaña, "Assessment of Supraharmonics Emissions in Low-Voltage Devices within the Frequency Range from 2 to 150 kHz," *2024 IEEE International Autumn Meeting on Power, Electronics and Computing (ROPEC)*, Ixtapa, Mexico, 2024, pp. 1-6, doi: 10.1109/ROPEC62734.2024.10877132.

[11] S. Sakar, S. Rönnberg and M. Bollen, "Interferences in AC–DC LED Drivers Exposed to Voltage Disturbances in the Frequency Range 2–150 kHz," in IEEE Transactions on Power Electronics, vol. 34, no. 11, pp. 11171-11181, Nov. 2019, doi: 10.1109/TPEL.2019.2899176.

[12] S. Sakar, S. K. Rönnberg and M. Bollen, "Interharmonic Emission in AC–DC Converters Exposed to Nonsynchronized High-Frequency Voltage Above 2 kHz," in IEEE Transactions on Power Electronics, vol. 36, no. 7, pp. 7705-7715, July 2021, doi: 10.1109/TPEL.2020.3047862.

[13] T. Tayjasanant, Wencong Wang, Chun Li and Wilson Xu, "Interharmonic-flicker curves," in *IEEE Transactions on Power Delivery*, vol. 20, no. 2, pp. 1017-1024, April 2005, doi: 10.1109/TPWRD.2004.838639.

[14] A. Gudiño-Ochoa, J. Jalomo-Cuevas, Jesús Ezequiel Molinar-Solís, and R. Ochoa-Ornelas, "Analysis of Interharmonics Generation in Induction Motors Driven by Variable Frequency Drives and AC Choppers," *Energies*, vol. 16, no. 14, pp. 5538–5538, Jul. 2023, doi: https://doi.org/10.3390/en16145538.

[15] B. Lu *et al.*, "Evolution analysis of wheel polygon wear considering the effect of interharmonics in electrical traction drive system," *Mechanism and Machine Theory*, vol. 191, p. 105470, Jan. 2024, doi: https://doi.org/10.1016/j.mechmachtheory.2023.105470.

[16] IEC61000-3-3, 2013, "Limitation of voltage changes, voltage fluctuations and flicker in public low-voltage supply systems, for equipment with rated current ≤ 16 A per phase and not subject to conditional connection".

[17] "IEEE Recommended Practice and Requirements for Harmonic Control in Electric Power Systems," in IEEE Std 519-2014 (Revision of IEEE Std 519-1992) , vol., no., pp.1-29, 11 June 2014, doi: 10.1109/IEEESTD.2014.6826459

[18] S. Elphick, S. Perera, and N. Browne, "Ripple signal amplification: measurement, modelling and mitigation," Figshare, Jan. 01, 2006. https://ro.uow.edu.au/articles/conference_contribution/Ripple_signal_amplification_measurement_modelling_and_mitigation/27800490?file=50572962

[19] Electromagnetic Compatibility (EMC) Part 2 2: environment Compatibility Levels for Low-Frequency Conducted Disturbances and Signalling in Public Low-Voltage Power Supply Systems, IEC 61000-2-2, Jun. 2017.

[20] A. D. Goswami, S. Chakraborty, B. Ghosh, J. Roy, and A. Naskar, "A laboratory based study on the effect of peripheral flickering LED sources on reaction time of drivers for object recognition," *Optik*, vol. 273, p. 170428, Feb. 2023, doi: https://doi.org/10.1016/j.ijleo.2022.170428.

[21] Jos Knockaert, C. Debruyne, and J. Desmet, "Interharmonics and LED flicker : an assessment by CFD," p. 4, Jan. 2019.

[22] O. Rahman, S. Elphick, K. M. Muttaqi and J. David, "Investigation of LED Lighting Performance in the Presence of Ripple Injection Load Control Signals," in IEEE Transactions on Industry Applications, vol. 55, no. 5, pp. 5436-5444, Sept.-Oct. 2019, doi: 10.1109/TIA.2019.2922291.

[23] H. Cao, T. Li, Y. Song, B. Zhu, X. Yang and C. Yuan, "Effect of Interharmonics on Flicker of Fluorescent Lamps," 2018 China International Conference on Electricity Distribution (CICED), Tianjin, China, 2018, pp. 585-589, doi: 10.1109/CICED.2018.8592497.

[24] R. Carbone, A. Lo Schiavo, P. Marino, and A. Testa, "Frequency coupling matrices for multi-stage conversion system analysis," European Transactions on Electrical Power, vol. 12, no. 1, pp. 17–24, Jan. 2002, doi: https://doi.org/10.1002/etep.4450120104.

[25] Á. Espín-Delgado, S. Rönnberg, S. Sudha Letha, and M. Bollen, "Diagnosis of supraharmonics-related problems based on the effects on electrical equipment," Electric Power Systems Research, vol. 195, p. 107179, Jun. 2021, doi: https://doi.org/10.1016/j.epsr.2021.107179.

[26] A. Novitskiy, S. Schlegel and D. Westermann, "Measurements and Analysis of Supraharmonic Influences in a MV/LV Network Containing Renewable Energy Sources," *2019 Electric Power Quality and Supply Reliability Conference (PQ) & 2019 Symposium on Electrical Engineering and Mechatronics (SEEM)*, Kärdla, Estonia, 2019, pp. 1-6, doi: 10.1109/PQ.2019.8818260.

[27] A. J. Collin, S. Z. Djokic, J. Drapela, R. Langella and A. Testa, "Light Flicker and Power Factor Labels for Comparing LED Lamp Performance," in *IEEE Transactions on Industry Applications*, vol. 55, no. 6, pp. 7062-7070, Nov.-Dec. 2019, doi: 10.1109/TIA.2019.2919643.

[28] A. M. Aboutaleb, A. Gholizad, J. Desmet and J. Knockaert, "Self-Induced and Mutual-Induced Emissions of Grid-Tied Converters," in IEEE Journal of Emerging and Selected Topics in Power Electronics, vol. 12, no. 4, pp. 3875-3886, Aug. 2024, doi: 10.1109/JESTPE.2024.3401255.

[29] A. J. Collin, S. Z. Djokic, J. Drapela, R. Langella and A. Testa, "Light Flicker and Power Factor Labels for Comparing LED Lamp Performance," in *IEEE Transactions on Industry Applications*, vol. 55, no. 6, pp. 7062-7070, Nov.-Dec. 2019, doi: 10.1109/TIA.2019.2919643.

[30] IEEE Recommended Practices for Modulating Current in High-Brightness LEDs for Mitigating Health Risks to Viewers," in IEEE Std 1789-2015 , vol., no., pp.1-80, 5 June 2015, doi: 10.1109/IEEESTD.2015.71186181

[31] K. R. Shailesh and T. Shailesh, "Review of photometric flicker metrics and measurement methods for LED lighting," 2017 4th International Conference on Advanced Computing and Communication Systems (ICACCS), Coimbatore, India, 2017, pp. 1-7, doi: 10.1109/ICACCS.2017.8014600.

[32] I. Castro, A. Vazquez, M. Arias, D. G. Lamar, M. M. Hernando and J. Sebastian, "A Review on Flicker-Free AC–DC LED Drivers for Single-Phase and Three-Phase AC Power Grids," in *IEEE Transactions on Power Electronics*, vol. 34, no. 10, pp. 10035-10057, Oct. 2019, doi: 10.1109/TPEL.2018.2890716.

[33] P. Erwin and P. Shackle, 2017, "Understand a new flicker metric and its application to ac-led light engines," LEDs-MAGAZINE

[34] Recommends, Assist. "Recommended metric for assessing the direct perception of light source flicker." *Assist Recommends* (2015): 1-18.

[35] EN 61000-4-19; Electromagnetic Compatibility (EMC). Part 4-19: Testing and Measurement Techniques—Test for Immunity to Conducted, Differential Mode Disturbances and Signalling in the Frequency Range 2 kHz to 150 kHz at a.c. Power Ports. CENELEC: Brussels, Belgium, 2014.

[36] IEC 61000-3-2; Electromagnetic Compatibility (EMC)—Part 3-2: Limits—Limits for Harmonic Current Emissions (Equipment Input Current ≤ 16 A Per Phase). IEC: Geneva, Switzerland, 2019.

[37] H. Markiewicz, A. Klajn, and W. University of Technology, "Standard EN 50160 Voltage Characteristics in Public Distribution Systems 5.4.2," 2004. [Online]. Available: www.lpqi.org.

[38] K. Skarżyński and A. Wiśniewski, "The reflections on energy costs and efficacy problems of modern LED lamps," Energy Reports, vol. 12, pp. 4926–4937, Nov. 2024, doi: https://doi.org/10.1016/j.egyr.2024.10.038.

[39] S. J. Lim, S. B. Oh and J. W. Jeon, "Efficiency Analysis of Lamp System: A Comparative Study of Domain E/E and Distributed Architectures," 2024 18th International Conference on Ubiquitous Information Management and Communication (IMCOM), Kuala Lumpur, Malaysia, 2024, pp. 1-6, doi: 10.1109/IMCOM60618.2024.10418346.

[40] M. L. Pay *et al.*, "A Review of LED Driver Topologies and Control Methods for Energy-Efficient Smart Farming Application," *Green energy and technology*, pp. 37–46, Jan. 2024, doi: https://doi.org/10.1007/978-3-031-55579-4_4.

[41] N. Nourani Esfetanaj, H. Wang, F. Blaabjerg and P. Davari, "Differential Mode Noise Prediction and Analysis in Single-Phase Boost PFC for the New Frequency Range of 9–150 kHz," in IEEE Journal of Emerging and Selected Topics in Industrial Electronics, vol. 3, no. 1, pp. 177-187, Jan. 2022, doi: 10.1109/JESTIE.2021.3066320.

[42] M. S. Osheba, A. M. Aboutaleb, J. Desmet, and Jos Knockaert, "The Impact of Grid Distortion on the Power Conversion Harmonics of AC/DC Converters in the Supraharmonic Range," Electronics, vol. 13, no. 12, pp. 2244–2244, Jun. 2024, doi: https://doi.org/10.3390/electronics13122244.

[43] S. King, "Luminous Intensity of an LED as a Function of Input Power," International School BangkokJournal of Physics, no. June, pp. 1–4, 2008

Marwa S. Osheba was born in Menoufia, Egypt, in December 1994. She received her B.Sc. (Hons.) and M.Sc. degrees in Electrical Engineering from the Faculty of Engineering, Menoufia University, Shebin El-Kom, Egypt, in 2017 and 2021, respectively. She is currently working towards her Ph.D. at Ghent University, Belgium. Her current research interests include power electronics converters, power quality, electromagnetic compatibility, and the investigation of supraharmonic issues.

Abdellatif M. Aboutaleb was born in Menoufia, Egypt, in Feb. 1993. He received the B.Sc. (hons.) and M.Sc. degrees in electrical engineering from the Faculty of Engineering, Menoufia University, Shebin El-Kom, Egypt, in 2016 and 2019, respectively. He is currently pursuing the Ph.D. degree with the Department of Electromechanical, Systems and Metal Engineering, Ghent University, Belgium. His main fields of interest include power electronics, power quality, electromagnetic compatibility, power filters, transmission line modelling and renewable energy. He currently serves as a reviewer for several leading conferences and journals including IEEE TRANSACTIONS ON POWER ELECTRONICS and IET RENEWABLE POWER GENERATION.

Jan Desmet (°1960) received the Polytechnical Engineer degree from the polytechnic academy in Kortrijk, the M.Sc. degree in Electrical Engineering from the V.U.Brussels and his PhD. degree at the K.U.Leuven, Belgium. Currently he is senior full professor at the Ghent University teaching Renewable Energy Sources and (µ)Grid integration.

His research interests include PQ, LV distributed generation, renewables, storage and hosting capacity. He is research leader of the research group EnSy/Lemcko of Ghent university. Besides his job as senior full professor and researcher, he also is member of several expert groups and both reviewer and topic chairman for international scientific conferences. He is also IEEE senior member, member of SC77A (IEC) and TC210 (CENELEC). His international scientific recognition is validated by his membership of the CIRED Technical Committee TC2 and several PhD juries abroad. Besides that, he was also member of the EASAC - 'Dedicated Storage on Electrical Power Systems' advisory board for the EU commission. Since November 2014, research group EnSy/Lemcko became member of the prestigious DERLab group. Jan Desmet is (co)author of more than 90 contributions published in international peer reviewed journals, 5 international technical reports and more than 100 conference papers. Finally he is also member of the academic board of the Belgium TSO ELIA, member of the strategic team for the Flemish DSO Fluvius and member of the steering group of Energy Transmission Competence Hub-ETCH

Jos Knockaert (M'09- SM'19) received the degree of industrial engineer in Electrotechnics in 1996 from the University College of Bruges-Ostend, the M.Sc. degree in Electronic System Design in 2001 from Leeds Metropolitan University and the Ph.D. degree in Engineering Science in 2009 from the K.U. Leuven. He worked as EMC-design engineer in the industry. He founded and is running the EMC laboratory in Ghent University, supporting companies in finding solution for EMI problems. Currently, he is associate professor with Ghent University, teaching electrical machines, electromagnetic compatibility and power electronics. He is member of the research group Lemcko with focus on high frequency problems in low voltage grids and industrial systems.